Deposition of Ga_2O_{3-x} ultrathin films on GaAs by e-beam evaporation

N. C. Oldham and C. J. Hill
T. J. Watson, Sr., Laboratory of Applied Physics, California Institute of Technology, Pasadena, California 91125

C. M. Garland
TEM Facility, W. M. Keck Engineering Laboratories, California Institute of Technology, Pasadena, California 91125

T. C. McGill[a)]
T. J. Watson, Sr., Laboratory of Applied Physics, California Institute of Technology, Pasadena, California 91125

(Received 8 October 2001; accepted 15 February 2002)

Gallium oxide films 20 Å in thickness were deposited onto GaAs substrates in ultra high vacuum (UHV) via e-beam evaporation from a monolithic high-purity source. The substrates were prepared by molecular-beam epitaxy and transferred to the oxide film deposition site in a wholly UHV environment. The Ga_2O_{3-x} films were probed by x-ray photoelectron spectroscopy (XPS). Chemical states were identified and stoichiometry was estimated. Metallic layers were deposited by e-beam evaporation in UHV after XPS analysis as caps and for future work. Film morphology and structure were probed by cross-sectional high-resolution transmission electron microscopy. The films were found to have $x \leqslant 0.3$ and a metal/oxide interface roughness <1 Å. © *2002 American Vacuum Society.* [DOI: 10.1116/1.1469011]

I. INTRODUCTION

Ultrathin films of Ga_2O_3 have attracted interest for use in applications including spin-dependent magnetic tunnel junctions[1] and compound semiconductor passivation.[2,3] Fabrication of these and similar Al_2O_3 films has been accomplished by oxidation of metallic layers in air[4] and by plasma.[5] Difficulties such as interlayer coupling[6] arising from substrate surface roughness and reduction of junction magnetoresistance because of underoxidation[7] have complicated the deployment of devices utilizing this technology. We present here a method for deposition, which exploits the high surface quality obtainable by molecular-beam epitaxy (MBE) as well as the reactivity of species deposited by electron-beam evaporation in ultrahigh vacuum (UHV) to obtain flat films with good stoichiometry. The depositions of Ni and Au cap layers are performed to demonstrate the suitability of this technique for two common overlayers.

In this work we describe our fabrication and characterization techniques for ultrathin Ga_2O_{3-x} films and analyze our results. We use high-resolution cross-sectional transmission electron microscopy (XTEM) and x-ray photoelectron spectroscopy (XPS) for analysis as these techniques are well suited for structural and chemical studies of layers of this type. Section II outlines the sequence and details of MBE deposition, e-beam evaporation, metal capping, and data analysis. Section III describes our measurements of oxide/metal interface roughness with XTEM and stoichiometry and film thickness with XPS. In Sec. IV we examine the role the surface structure of the GaAs substrate plays in the resultant oxide film chemistry as well as compare our results to previous work in the literature. Section V reiterates our findings.

II. EXPERIMENT

Commercially available p-GaAs wafers (GaAs:Zn, $N_A = 5\times10^{18}$ cm^{-3}) were In bonded to Mo blocks for MBE growth. Oxides were desorbed at 600 °C in UHV. (See Fig. 1 for a schematic of our system.) Layers of additional GaAs were grown on these wafers in a Perkin–Elmer 430 MBE chamber. All growths were performed in an excess flux of cracked As and Be was used as the p-type dopant instead of Zn.

Three growths were performed (see Table I). These were monitored by reflection high energy electron diffraction (RHEED) during growth and were found to have bright, streaky patterns during postgrowth cooling to room temperature. The difference in reconstruction arose due to the fact that sample I was removed from the As flux during cooling, while sample II was kept in the As flux down to lower tem-

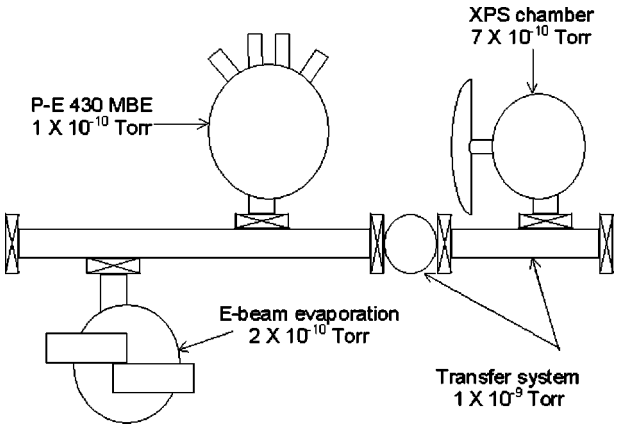

FIG. 1. Schematic of relevant elements of the UHV system used in this work and their base pressures.

a)Author to whom correspondence should be addressed; electronic mail: tcm@ssdp.caltech.edu

TABLE I. GaAs buffer layers.

Sample	Growth temperature (°C)	Doping	Final reconstruction
I	575	none	(2×4)
II	550	Be, 3×10^{-18} cm^{-3}	(4×4)

perature (150 °C). The stoichiometry of the surface region of these buffer layers is summarized in Table II where it is seen that sample I, having a (2×4) surface, is As rich, whereas sample II, having a (4×4) surface, is As poor.

After growth, these samples were transferred in UHV conditions to a Physical Electronics (Phi) Model 5600 MultiTechnique analysis chamber for XPS. The chamber is equipped with Mg $K\alpha$ and monochromated Al $K\alpha$ emission sources; both were used in this study. Angle-resolved scans are possible only with the Mg anode due to chamber geometry. The chamber uses a Phi Model 10-360 hemispherical analyzer and position-sensitive detector (minimum resolution 0.6 eV). The pass energy was 187.85 eV and the step size 0.8 eV regardless of anode.

After preliminary XPS analysis, the samples were transferred in UHV to the e-beam evaporation chamber for oxide film deposition. The e-beam evaporation chamber is a custom model equipped with two 3 kW Thermionics guns. The wafers were heated to 300 °C prior to activation of the e beam.

The sources for growth were high-purity (99.995% metals basis) sintered lumps of Ga_2O_3, obtained commercially. No oxygen was provided during evaporation of Ga_2O_3 except that liberated by evaporation of the source, which was sufficient to elevate chamber pressure to 2×10^{-6} Torr. This is very similar to that reported by Hong *et al.*[8] who utilized e-beam evaporation from a $Gd_3Ga_5O_{12}$ source.

During evaporation the source did not seem to melt, but rather seemed to decompose in a localized manner as the electron beam was seen to bore holes into the source. Deposition rates were controlled by adjustment of the e-beam current and were in the range 0.1–0.2 Å/s. Film thickness was controlled by a quartz crystal monitor (QCM), according to which the oxide growths were 22 Å thick.

Following evaporation, the chamber pressure was seen to decrease below 5×10^{-9} Torr within minutes as the substrate cooled. The specimens were returned in UHV to the analysis chamber, where XPS was used to probe the surface chemistry of the oxide film. Multiple scans of each film were completed, and these are discussed in Sec. III.

Following XPS, both samples were capped with metallic layers in the e-beam evaporation chamber. The substrates were at room temperature. Sample I was capped with 175 Å of Au; sample II was capped with 1000 Å of Ni.

At this point, the samples were removed from UHV and cleaved to obtain portions for XTEM. These were thinned by polishing, dimpling, and low-voltage, low-angle ion milling and examined in a Philips EM430 TEM with a LaB_6 crystal operating at a voltage of 300 kV.

TABLE II. Results of XPS probing of GaAs buffer layers prior to oxide film deposition. Elemental intensities are obtained by dividing observed 3*d* peak areas by atomic sensitivity factors.

	I Mg $K\alpha$	I Al $K\alpha$	II Mg $K\alpha$	II Al $K\alpha$
I_{Ga}	29 672	8889	42 749	10 133
FWHM[a] (eV)	2.4	2.3	2.5	2.4
I_{As}	35 173	10 535	41 462	9465
FWHM (eV)	2.6	2.5	2.6	2.5
Observed As:Ga ratio	1.185	1.185	0.970	0.934

[a]Full with half maximum.

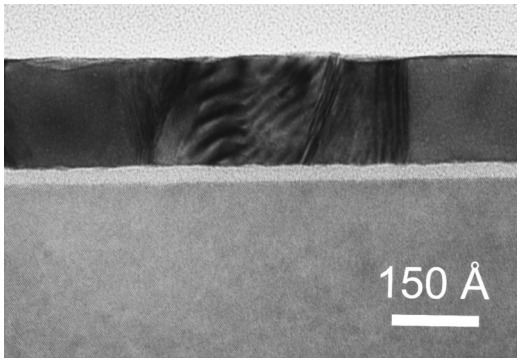

FIG. 2. XTEM photomicrograph of sample I. The bottom layer is the intrinsic GaAs buffer layer. The topmost layer is the 175-Å-thick Au cap. Between these layers, the 20-Å-thick Ga_2O_{3-x} layer is seen to be distinct and fairly smooth.

III. EXPERIMENTAL RESULTS

A. XTEM

Figures 2 and 3 show samples I and II at a lower magnification. The polycrystalline metal caps and the epitaxial, nearly defect-free nature of the GaAs buffer layers are evident. The metallic layers appear to evidence a large number of grain boundaries and other defects typical of metals deposited onto substrates at room temperature. At higher mag-

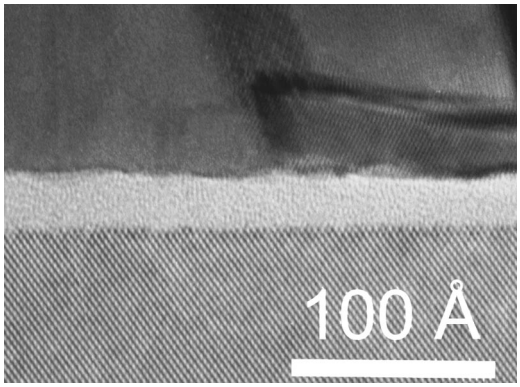

FIG. 3. XTEM photomicrograph of sample II, 1000 Å Ni/20 Å Ga_2O_{3-x}/p-GaAs.

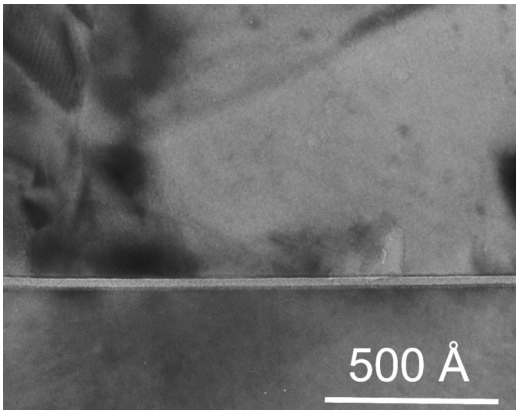

FIG. 4. High-magnification XTEM photomicrograph of sample I. Some interdiffusion between the oxide and Au layers is evident. This sample appears to have no long-range order but non-negligible short-range order.

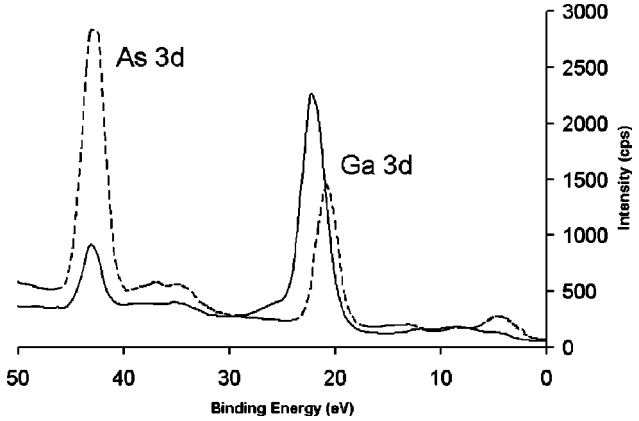

FIG. 6. XPS scans of sample I before and after e-beam evaporation of Ga_2O_3. The dashed line represents the GaAs surface prior to evaporation, the solid line the sample surface after oxide film deposition.

nification, atomic-level features are readily evident (Figs. 3 and 5). Limited interdiffusion appears to have occurred but the outlines of the layers are still distinct.

Visual analysis of Figs. 3 and 5, followed by fitting points on the metal/oxide interface to a sinusoidal function using a Texas Instruments TI-86, yielded root-mean-square (rms) roughness <0.5 Å. Roughness wavelengths were 66 and 39 Å, respectively. Analysis of other images confirmed that the rms roughness of the interface is <1 Å. The values of wavelength obtained are somewhat arbitrary given the low roughness values.

An attempt was made to collect selected-area or transmitted-electron diffraction data, but due to the large sampling area (0.5 μm diameter) of our smallest aperture, the signal from the oxide layer cannot be isolated with certainty from those of the GaAs buffer layer and the multiple metal grains in each cap or diffusion of the transmitted beam.

B. XPS

Precise identification of the chemical states in the Ga–As–O system with XPS has been difficult with similar but ambiguous reports emerging from the literature.[9–15] Much of this is due to variance in instrument resolution and sensitivity. Our deposition of relatively large amounts of Ga and oxygen on the surface restricts the likely number of compounds considerably, simplifying analysis.

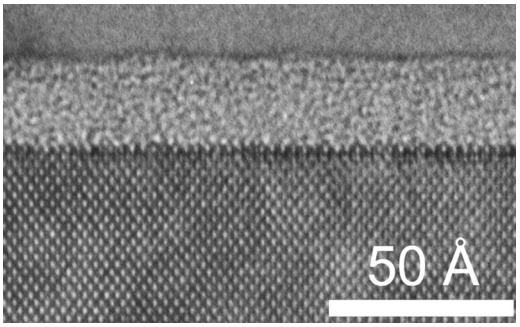

FIG. 5. High-magnification XTEM photomicrograph of sample II. The initial adatoms of the oxide appear to exhibit a preference for a particular site, but subsequent layers seem to have no long-range ordering and little short-range order. Sample I appears to have better bonding between the oxide and GaAs layers (see Fig. 4), likely due to its greater concentration of oxygen.

The $3d$ transition in Ga is preferred for chemical state identification due to smaller offsets in the more prominent $2p_{3/2}$ transition. Figure 6 shows the $3d$ transitions in both As and Ga before and after oxide film deposition. Data in this figure were not processed for background noise reduction. The As peak is suppressed without shift while the Ga $3d$ transition undergoes a dramatic change in area and shape. This is consistent with the addition of Ga in the Ga_2O_3 state as the transition in this state is approximately 1.2 eV higher than that of Ga in the GaAs state.[15]

An angle-resolved scan of sample II was performed at four angles for careful identification of Ga bonding states. The fit was performed for two peaks. These are believed to be the binary oxide and arsenide states of Ga. The other Ga-bearing compounds listed by Hollinger *et al.*[15] are very oxygen rich and are thus very unlikely to be formed in the deposition events described here. The fits are seen in Fig. 7. The values of χ^2 are listed in Table III. The peak offset varied from 1.0 to 1.2 eV.

It is possible to use these data to estimate the thickness of the oxide film. Using the method of Tanuma, *et al.*[16] the inelastic mean-free path Λ of electrons at 1230 eV (the energy of the Mg $K\alpha$ transition minus a binding energy of roughly 20 eV) inside Ga_2O_3 is most nearly 24.2 Å. Peak area data are summarized in Table III. These data were fit to the linear attenuation equation

$$I(\theta) = I_0 \exp\left(-\frac{d}{\Lambda \sin(\theta)}\right), \tag{1}$$

where θ is the take-off angle (the angle between the detector axis and the plane of the sample surface) and d is the surface layer (in this case, Ga_2O_{3-x}) thickness. The linear regression yielded $d = 19.6$ Å with $R^2 = 0.807$, which is in accord with both the QCM and the XTEM photomicrographs.

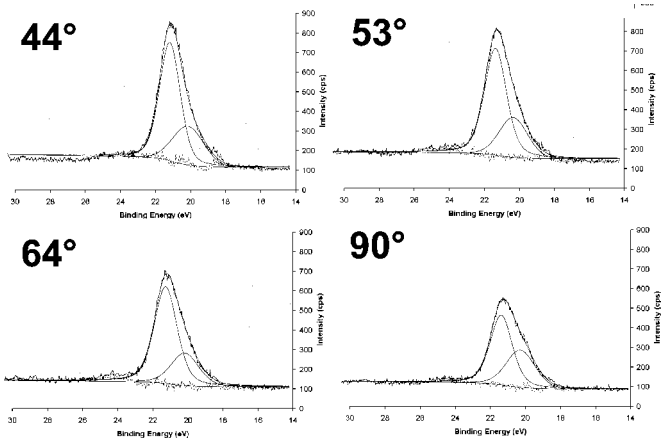

FIG. 7. Deconvolution of the Ga $3d$ transition in sample II measured by an angle-resolved scan using a Mg $K\alpha$ source; see Table III. The rightmost (lower-energy) curves are presumed to originate from Ga bonded to As, while the leftmost (higher-energy) curves are presumed to originate from Ga bonded to O.

To measure the stoichiometry of the film, peak areas were measured from full spectral scans. Background noise was removed with a Shirley algorithm. Measured peak areas were divided by atomic sensitivity factors obtained from Phi for our specific instrumentation to obtain atomic concentrations. See Table IV for the results of this analysis.

IV. DISCUSSION

The XTEM photomicrographs suggest a smooth oxide film layer with an indeterminate structure. The thinness of the layer makes both x-ray and electron diffraction studies difficult. *In situ* measurement using RHEED would be of considerable value in structural studies but the absence of this tool on our e-beam evaporation chamber would not permit such examination during growth. An amorphous structure was claimed by Hong *et al.* for $(Ga,Gd)_2O_3$ films[8] using RHEED and TEM for characterization and this is evidently the case here as well. Given the differences in symmetry and unit cell size between GaAs ($F\bar{4}3m$, $a=5.65$ Å) and the stable phase of Ga_2O_3 (β-Ga_2O_3, $C2/m$, $\beta=103.7°$, $a=12.2$ Å, $b=3.04$ Å, $c=5.80$ Å), it is unlikely that epitaxy of Ga_2O_3 would be realized under these conditions.

As seen in Figs. 4 and 5, bonding between GaAs and Ga_2O_{3-x} at their interface seems to be uniform and consistent. There appears to be some site preference for the initial adatoms of the evaporated material, which is in accord with the hypothesized interface predicted by Hong *et al.*[17] Several factors point to the likelihood that these are predominantly oxygen adatoms attaching to Ga. The standard-state Gibbs free energy of formation at 300 °C for GaAs is -110 kJ/mol; that of $\frac{1}{2}Ga_2O_3$ is -570 kJ/mol.[18]

Since we see that both films are slightly underoxidized, we conclude that most likely the structure consists of clusters of Ga with adsorbed oxygen similar to that of underoxidized Fe on α-Al_2O_3 as described in Fig. 3(d) of Chambers' review of thin-film oxide epitaxy.[19] Given that XPS apparently reports the presence of Ga in the Ga_2O_3 chemical state ($Ga_{Ga_2O_3}$), we thus speculate that the short-range structure seen by Ga atoms in the oxide film is similar to that of β-Ga_2O_3 (Ga in four- and six-oxygen complexes,[15] along with some free Ga), with no long-range structure that may be positively identified from our data. Sample I (Fig. 4) appears to evidence more short-range order than sample II, likely due to the smaller value of x for sample I. The difference in stoichiometry is possibly due to the different surface reconstructions of the substrates (Table I). Tentatively, it seems a As-terminated (2×4) reconstruction may give a better film.

The values of roughness and wavelength calculated in Sec. III would seem to compare favorably to the rms roughness of 7.3 Å and wavelength of 94 Å estimated by Schrag *et al.*;[6] however, those workers used a measurement of the Néel coupling field for quantitative analysis and direct comparison may be misleading.

It is seen from the data in Table IV that the amount of As in the XPS sampling region is considerably less than the Ga assumed to be in a Ga–As bond (Ga_{GaAs}). Thus it seems apparent that As is being lost from the upper layers of GaAs during oxide deposition possibly by surfactant action, gas-phase desorption, or both. Instead of a Ga_{GaAs} state, the lower energy peak in the deconvolutions of the Ga $3d$ transition may represent free Ga. This would appear to contradict the XTEM photomicrographs; Figs. 2–5 imply that a nearly pristine GaAs layer persists up to the oxide/GaAs interface. Inspection of the photomicrographs implies some small increase in the defects in the substrate monolayers closest to the interface, but it is uncertain if this would account for the dramatic nonstoichiometry observed with XPS. Further investigation is required.

Exact determination of the energy shift would aid in the

TABLE III. Angle-resolved intensity data obtained from the curves in Fig. 7.

Take-off angle	$Ga_{Ga_2O_3}$ Area (arbitrary)	$Ga_{Ga_2O_3}$ FWHM (eV)	Ga_{GaAs} Area (arbitrary)	Ga_{GaAs} FWHM (eV)	χ^2	$\frac{I_{GaAs}}{I_{GaGa_2O_3}}$
44°	1009	1.55	317	2.02	1.170	0.31417
53°	923	1.53	291	1.96	1.362	0.31528
64°	839	1.61	312	1.93	1.371	0.37187
90°	714	1.51	322	1.96	1.487	0.45098

TABLE IV. Intensities of Ga, As, and O peaks for stoichiometry estimation.

Transition	I Mg $K\alpha$	I Al $K\alpha$	II Mg $K\alpha$	II Al $K\alpha$
$Ga_{Ga_2O_3}$ $3d$	61 298	10 988	64 193	9819
Ga_{GaAs} $3d$	34 431	8533	33 724	6807
As $3d$	5316	1967	4052	988
O $1s$	90 153	16 367	87 321	13 570
$\frac{2I_O}{I_{GaGa_2O_3}}$	2.9415	2.9791	2.7206	2.7639
$\frac{I_{As}}{I_{GaGaAs}}$	0.1544	0.2305	0.1201	0.1451

solution of this problem. Unfortunately, it is difficult to determine the shift using the traditional C $1s$ transition since a Ga Auger emission ($L_3M_{23}M_{45}$) nearly coincides with and in some cases overlaps the C $1s$ peak whenever nonmonochromated Mg $K\alpha$ x rays are used, and the C $1s$ peak is almost undetectable for most of our samples due to the clean nature of the UHV process. There does not seem to be any As–O compound formation as the O $1s$ – As $3d$ separation is 490.0 eV for both samples I and II when scanned with monochromated Al $K\alpha$ x rays. This is $\geqslant$3.5 eV larger than the separation seen in any of the As–O or Ga–As–O compounds studied by Hollinger *et al.*[15] Therefore, the chemistry of the substrate layers nearest the oxide film remains to be exactly resolved.

There was some concern regarding diffusion of the metallic overlayers into the Ga_2O_{3-x} films, as it is necessary to briefly (approximately 5 min) heat the samples to the melting point of In (157 °C) to debond them from the Mo blocks after exiting from the vacuum. As mentioned above, limited interdiffusion does seem to occur, but this does not meaningfully compromise the integrity of the oxide film. The Ga_2O_3/GaAs interface seems to be robust.[3]

It has been suggested that optimal tunneling properties may be found with thinner junctions and upon annealing[1,7] in ferromagnet/insulator/ferromagnet structures. This is due to competing effects, namely oxidation of the neighboring layers and the formation of metallic paths in the junction layer. As these would also be expected to be difficulties in structures involving a semiconductor in place of a metal, it is expected that future investigations of these parameters will be of importance. Both the XTEM and XPS techniques are well suited for materials studies of such ultrathin films.

V. CONCLUSION

We have fabricated Ga_2O_{3-x} films with $x \leqslant 0.3$ in UHV by e-beam evaporation from a high-purity monolithic source. Deposition on epitaxial GaAs buffer layers yields very smooth films suitable for the growth of metallic overlayers with rms interface roughness <1 Å. Film properties have been examined qualitatively and quantitatively with XPS and XTEM. This deposition technique seems to be extendable to numerous applications utilizing oxide tunnel junctions.

ACKNOWLEDGMENTS

The authors would like to acknowledge Professor J. O. McCaldin for his contribution of background information and suggestions throughout this project as well as E. J. Preisler and R. A. Beach for their assistance with XPS.

[1]Z. Li, C. de Groot, and J. H. Moodera, Appl. Phys. Lett. **77**, 3630 (2000).
[2]M. Passlack *et al.*, J. Appl. Phys. **77**, 686 (1995).
[3]M. Passlack, M. Hong, J. P. Mannaerts, S. N. G. Chu, R. L. Opila, and N. Moriya, Proceedings International Electronics Devices Meeting, 1995, Session 15, paper 6.1, p. 383.
[4]T. Miyazaki and N. Tezuka, J. Magn. Magn. Mater. **139**, L231 (1995).
[5]W. Zhu, C. J. Hirschmugl, A. D. Laine, B. Sinkovic, and S. S. P. Parkin, Appl. Phys. Lett. **78**, 3103 (2001).
[6]B. D. Schrag, A. Anguelouch, G. Xiao, P. Trouilloud, Y. Lu, W. J. Gallagher, and S. S. P. Parkin, J. Appl. Phys. **87**, 4682 (2000).
[7]J. S. Moodera, J. Nassar, and G. Mathon, Annu. Rev. Mater. Sci. **29**, 381 (1999).
[8]M. Hong, M. Passlack, J. P. Mannaerts, J. Kwo, S. N. G. Chu, N. Moriya, S. Y. Hou, and V. J. Fratello, J. Vac. Sci. Technol. B **14**, 2297 (1996).
[9]G. Leonhardt, A. Berndtsoon, J. Hedman, M. Klasson, and R. Nilsson, Phys. Status Solidi B **60**, 241 (1973).
[10]L. Ley, S. P. Kowalczyk, F. R. McFeely, R. A. Pollak, and D. A. Shirley, Phys. Rev. B **8**, 2392 (1973).
[11]H. Iwakuro, C. Tatsuyama, and S. Ichimura, Jpn. J. Appl. Phys., Part 1 **21**, 94 (1982).
[12]H. Iwasaki, Y. Mizokawa, R. Nishitani, and S. Nakamura, Surf. Sci. **86**, 811 (1979).
[13]I. Lindau, P. Pianetta, C. M. Garner, P. E. Chye, P. E. Gregory, and W. E. Spicer, Surf. Sci. **62**, 45 (1977).
[14]Y. Mizokawa, H. Iwasaki, R. Nishitani, and S. Nakamura, J. Electron Spectrosc. Relat. Phenom. **14**, 129 (1978).
[15]G. Hollinger, R. Skheyta-Kabbani, and M. Gendry, Phys. Rev. B **49**, 11159 (1994).
[16]S. Tanuma, C. J. Powell, and D. R. Penn, Surf. Interface Anal. **11**, 577 (1988).
[17]M. Hong, A. R. Kortan, J. Kwo, J. P. Mannaerts, J. J. Krajewski, Z. H. Lu, K. C. Hsieh, and K. Y. Cheng, J. Vac. Sci. Technol. B **18**, 1688 (2000).
[18]*CRC Handbook of Chemistry and Physics*, edited by D. R. Lide (Chemical Rubber Corp., Boca Raton, FL, 1994), Chap. 5.
[19]S. A. Chambers, Surf. Sci. Rep. **39**, 105 (2000).